

EFFECTS OF MICROSTRUCTURE ON THE FRACTURE TOUGHNESS OF METALLIC ALLOYS

J. F. Knott

Department of Metallurgy and Materials Science, University of Cambridge, Cambridge, England

ABSTRACT

The paper contains an account of the use of micro-mechanistic modelling to relate macroscopic fracture toughness values to an alloy's microstructure and deformation characteristics. The fracture modes treated in detail are transgranular cleavage, void growth and "fast shear". In each case, attention is paid to the distribution and morphology of carbide particles and to the role played by non-metallic inclusions. For wrought steels, transgranular cleavage is dominated by carbides, but in weld metals, critical microcracks may be initiated by the fracture of oxide or duplex inclusions. In low strength alloys, fibrous fracture is dominated by weakly-bonded, non-metallic inclusions, but in clean, high-strength structural alloys, the linkage between voids is dominated by the strength and interfacial cohesion of carbides or intermetallic hardening particles. Effects of stress-state on the fracture processes are discussed briefly.

KEYWORDS

Transgranular cleavage; microcracks; carbides; inclusions; dislocations; interfacial cohesion; stress-state.

INTRODUCTION

It is useful to categorise a fracture process either as a cracking process or a rupture process. Cracking is associated with fast, unstable propagation, substantially controlled by the local tensile stress, and is associated with transgranular cleavage or intergranular decohesion. Rupture is often associated with void growth and coalescence and, in low strength alloys, is largely controlled by a combination of matrix strain and triaxial stress. In high-strength alloys, however, "fast shear" may induce premature linkage of expanding voids and, in some circumstances, it is possible that micro-cracking of small, second-phase particles contributes to the rupture process. The effects of stress-state then depend critically on the fine details of the "fast shear" component.

In the present paper, an account is given of recent developments in the

modelling of cracking and rupture processes, showing how quantitative links with macroscopic toughness values may be derived. Particular attention is paid to mechanisms which operate in alloys utilised in energy and transportation industries and the opportunity is taken to highlight recent research at Cambridge involved with C-Mn weld-metals, as used in pipelines, off-shore oil rigs and generally in construction engineering; A533B/A508 steels used in PWR pressure vessels; HY steels, used in naval and submersible applications; and a variety of high strength/weight alloys (HSLA, 300M, maraging steels; 7000 series AlZnMgCu alloys) used in aerospace applications. Comments are made on the sources of scatter in toughness values, with reference to work on dual-phase steels, and the final section of the paper treats behaviour in testpieces containing short, through-thickness or semi-elliptical cracks, representative of defects in service. Intergranular fracture mechanisms are not treated, because they form the subject of another plenary review (McMahon 1984), but attention should be drawn to effects on stress-relief-cracking and, particularly, to the occurrence of dynamic segregation to the region ahead of a growing crack tip (Hippesley et al. 1982).

TRANSGRANULAR CLEAVAGE

The onset of catastrophic crack propagation in an annealed mild-steel microstructure (comprising ferrite grains and grain-boundary cementite, Fe_3C) is controlled by the attainment of a critical tensile stress, σ_F , in the yielded zone ahead of a notch or pre-crack. The yielded zone is necessary to nucleate cracks in the cementite by dislocation arrays. Experimentally, the value of σ_F is found not to vary significantly with temperature (Knott 1966) or, by inference, with strain-rate (Knott 1967a) if fracture is initiated by slip, although initiation by mechanical twinning induces temperature dependence (Oates 1967). Further results show that σ_F is relatively insensitive to neutron irradiation (Fearneough 1972) but exhibits modest increases with uniform prestrain (Knott 1967b, Groom and Knott 1975, Pineau 1981). Following metallographic studies made by McMahon and Cohen (1965) in tensile specimens, which showed that microcrack nuclei formed in grain-boundary carbides, a rigorous crack propagation model was developed by Smith (1966) to relate values of σ_F to the grain-boundary carbide thickness, C_0 , and "plastic work-of-fracture", γ_p , through the expression

$$\sigma_F^2 C_0 + (k_Y^S)^2 \{1 + (4/\pi)(\tau_i/k_Y^S) C_0^{1/2}\}^2 = 4E\gamma_p/\pi(1-\nu^2) \quad (1)$$

where E is Young's modulus, k_Y^S is the slope of the Petch plot in shear, and τ_i is the friction stress.

The main features of this expression have been discussed previously (Knott 1977, 1982a). The apparent lack of dependence on grain size is met by the fact that heat-treatments which consist of simple cooling from austenite give increased values of C_0 for increased values of d (Curry and Knott 1978). The lack of temperature dependence of γ_p , as inferred from experimental values of σ_F , combined with its "best fit" value, for the "coarsest observed" or 95th percentile carbide thickness, of $14Jm^{-2}$ (Curry and Knott 1979), which is approximately seven times the elastic work of fracture, may be reconciled in terms of the (virtually athermal) generation and local movement of crack-tip dislocations which, in iron, assist the bond-separation process by facilitating larger atomic displacements than would be possible in elastically stiff surroundings. It should be noted that the Griffith criterion itself

treats "before" and "after" states in an energy balance, but does not consider any "activation energy" associated with the postulated intermediate state necessary to operate the mechanism which enables the system to change from "before": strained bonds; to "after": two separated surfaces (Knott 1982).

The expression in (1) also assumes that there is a single, deterministic value of carbide thickness, C_0 . In a real steel, there are distributions both of thickness, C_0 , and of the angle that a carbide of given thickness makes with the line of action of the local tensile stress. The experimental values of σ_F under constant test conditions should therefore be distributed statistically, although the combination of the two separate distributions (of thickness and of angle) is difficult to treat in a quantitative manner. A more straightforward microstructure is that of spheroidal carbides in a ferritic matrix and, here, Curry and Knott (1978) were able to show that values of σ_F , based on the 95th percentile radius, were compatible with the same value of γ_p , $14Jm^{-2}$, as that found to give the "best fit" results for grain-boundary carbides. The propagation was modelled in terms of a Griffith criterion, modified to take account of "penny shaped" microcracks.

The basic principle underlying the relationship between σ_F and a material's fracture toughness may be appreciated in simple terms by considering the distribution of local tensile stress, $\sigma(r)$ ahead of a pre-crack. Under LEFM conditions, this is given by:

$$\sigma(r) = K/(2\pi r)^{1/2} + \dots \text{series} \quad (2)$$

or, by rearrangement

$$K = \sigma(r) (2\pi r)^{1/2} \quad (3)$$

In a microstructure containing a uniform distribution of carbides of identical size, it is then possible approximately to regard K_{IC} as the value of applied stress intensity required to generate the critical tensile stress at the site of a microcrack nucleus. If this were situated at a distance r^* ahead of the crack tip, the critical condition for fracture would be $\sigma(r^*) = \sigma_F$, i.e.

$$K_{IC} = \sigma_F (2\pi r^*)^{1/2} \quad (4)$$

This LEFM form does not hold for structural metals, because it is necessary to produce a plastically deformed region ahead of the precrack to nucleate cleavage microcracks. Although a full analysis (RKR) can be carried out using finite element elastic/plastic solutions (Ritchie, Knott and Rice 1973) or assuming power-law hardening (Curry 1978), the concept of a "critical distance", r^* , remains, however, unchanged. The main difference is that the value of $\sigma(r^*)$, at a fixed distance r^* , increases not only with plastic zone size (applied stress intensity) but also as a simple multiple of uniaxial yield stress, σ_Y , for a given size of plastic zone. If σ_F is substantially independent of temperature or its temperature dependence has been determined, in separate notched-bar experiments, it becomes possible to predict the temperature dependence of K_{IC} , knowing that of yield stress. Additionally, it is possible to predict shifts in the K_{IC} transition curve induced by increases in yield stress due to strain ageing, neutron irradiation (Ritchie, Serverand Wullaert 1979) or increased strain-rate (Costin and Duffy 1979).

The argument so far assumes that a single value may be attributed to σ_F (i.e. that all carbides are of the same size) and that r^* is also constant. In real microstructures, there are distributions of both size and spacing. If

a constant value of σ_F is obtained from notched bar tests and measurements of K_{IC} are made at the same temperature, it is possible, from the elastic/plastic equivalent of equation 4) to calculate a parameter, \bar{x} , having dimensions of length, which might be regarded as a "characteristic distance", corresponding to the location of carbides in which critical cleavage micro-crack nuclei form. Ritchie, Knott and Rice (1973) found that \bar{x} , in the steel they studied, was almost exactly equal to two grain diameters, but it was shown later (Curry and Knott 1976) that this relationship did not hold generally for a range of grain sizes. In their study of cleavage fracture in spheroidised microstructures, Curry and Knott (1979) attempted to take the full distributions of carbide size and spacing into account and to relate values of σ_F to values of K_{IC} by a probabilistic treatment. First, it was necessary to determine, using quantitative metallography, the histogram of the probability per unit volume, $N(x)$, that a carbide would have a given radius x (where x is the mean value in a size bin). Secondly, it was possible to make use of the previously determined relationship between σ_F and $x^{-1/2}$ to obtain appropriate values of σ_F for these mean values of x . Thirdly, by considering an element of area at a position (r, θ) ahead of a precrack subjected to a given applied stress intensity K , the magnitude of the local tensile stress $\sigma(r)$ could be determined. The value of $\sigma(r)$ was then compared with the distribution of σ_F values for that element and a fractional failure probability could be deduced and summed for all elements. As the applied value of K is increased, the value of this sum also increases and failure was assumed to occur when the sum reached unity.

The model is two-dimensional in nature, but nevertheless gave good agreement with experimental results for different temperatures and carbide spacings for constant input parameters, such as γ_p and geometrical factors. It is interesting to note that it is unnecessary to determine details of the carbide size distribution when the sizes are small ($< 0.1\mu\text{m}$) because the values of σ_F are then so high that they could not be achieved even at -160°C using the maximum stress intensification available from the triaxial stresses in the plastic zone (approx. $4\sigma_y$). Cleavage fracture might still be produced at -196°C , but would have to be initiated by twinning, rather than by slip. A second point is that it is also assumed that there are equal chances of sampling the full carbide distribution in the relatively steep stress gradient ahead of a precrack and in the more uniformly stressed area ahead of a notch. If this assumption does not hold, natural scatter is induced in K_{IC} values (on the basis of a 2-D model). The effect should not be significant for small carbides, but may be of importance for coarser micro-fracture units and is discussed below, in connection with quenched-and-tempered structural steels. For simple spheroidal microstructures, the statistical model has been generalised by Evans and Hutchinson (1983) who assume a Weibull distribution of carbides (rather than a measured distribution) in association with the power-law hardening stress analysis and has been combined with a temperature dependent $\gamma_p(\sigma_F)$ term by Wallin, Saario and Törönen (1984).

Having described the importance of the carbide size distribution with respect to the transgranular cleavage fracture of wrought, low-carbon steels, it is of interest to examine the recent results obtained by Tweed and McRobie (Tweed and Knott 1982, 1983; McRobie and Knott 1984) for as-deposited C-Mn weld metals. Here, the microstructures are composed of "grain-boundary" ferrite, which nucleates on prior austenite grain boundaries and grows by diffusion, driving carbon ahead of the ferrite/austenite interface, and "acicular" ferrite. This nucleates independently on (silicate and oxide) deoxidation products which are present as a relatively high volume fraction of small (usually $< 2\mu\text{m}$ diameter) inclusions. Cleavage cracks propagate more

easily in the grain boundary ferrite than in acicular ferrite, but the thickest carbides are to be found in between the acicular "grains", so that the microstructural features controlling the toughness of the as-deposited material were not clear a priori. By a detailed study of fracture surfaces, Tweed and McRobie have demonstrated that, in many cases, the critical micro-crack nuclei form on non-metallic inclusions (see Fig. 1). These observations were supported by fracture mechanics calculations applied to the micro-structural components, which showed that a "penny-shaped" crack could propagate from a (large) inclusion at a stress lower than that required to propagate a crack from a (thin) carbide. The toughness values could be related to features of the "deoxidation product" size distribution, but it was also noticed that occasional, particularly poor, results were associated with the presence of (a second distribution of) large, exogenous (Ca-bearing, K-bearing) inclusions, which had presumably entered the liquid weld-pool directly from the electrode coating. Again, causes of scatter are clear and elimination of such large inclusions has been shown to give improved, consistent, toughness values in C-Mn weld deposits (Judson and McKeown 1982). The benefits of this close control on inclusion distribution will presumably be greater when the carbon content is low, and carbides are thin, than when it is high, because carbides may then serve as the more important crack nuclei.

The σ_F criterion and RKR model have been examined for a number of other microstructures. Following earlier work by Evensen et al (1977), Shehata and Boyd (1982) studied behaviour in controlled-rolled pipeline steel, which consists generally of fine ferrite grains and thin grain-boundary carbides or other non-ferritic products. Due to non-uniformity of processing, however, occasional coarse ferrite grains (and, presumably, coarse carbides) may be found in the microstructure and it is the distribution of these that effectively controls the cleavage fracture. Since cooling-rate is critical, processing features such as intermediate hot-coiling which give economic savings through energy conservation, need to be examined carefully. Additionally, grain coarsening combined with strain-ageing, in heat-affected-zones in welded pipelines must be assessed in terms of its possible effects on cleavage fracture resistance.

Strain-ageing is an important factor with respect to a steel's resistance to cleavage fracture in service. It may result either from mechanical, cold work followed by ageing or from thermal strains produced during the cooling of each pass in a welded joint. The value of σ_F is increased by prestrain, but the effective value of yield stress is also raised by the combination of strain and ageing, with the net result that smaller plastic zones (lower stress intensifications) are required to produce the critical value, so that the notch- or crack tip-ductility is reduced. The strength of the effect is demonstrated by results obtained by McRobie, in his examination of factors affecting the toughness of the "root run" in a multipass C-Mn steel weld deposit. Even in grain-refined material (average grain size $5\mu\text{m}$), three successive uniform prestrains of 2%, each followed by an ageing treatment of 30 mins at 230°C are sufficient to change the fracture mode in small, pre-cracked C.O.D. testpieces at -10°C from fibrous to cleavage, with an accompanying change in the load: clip-gauge displacement curve from a " δ_m " type to a " δ_c " type (Fig. 2). Similar behaviour is observed for as-deposited microstructures, although these are not initially so tough, and it must be concluded that quite severe embrittlement can be developed in regions of a weld that have been subjected to strain-ageing. These regions are, of course, also harder, so that higher stresses are needed to produce plastic flow in them than in non-strain-aged material.

The other main class of steels in general structural use is quenched and tempered, including compositions such as A533B/A508; HY80, HY130; $2\frac{1}{2}\text{Cr1Mo}$. The M_s temperatures for such steels are high - in the range 300°C to 400°C - and the as-quenched microstructures consist of "packets" of martensitic laths, containing a fine distribution of auto-tempered carbides (Dolby and Knott 1972; Bowen and Knott 1984). Similar structures would be expected in the HAZ, following welding, although, if preheat is applied, the microstructure may be bainitic (Dolby and Knott 1972; Hippsley, Knott and Edwards 1980). On tempering at temperatures around 350°C , the intra-lath carbides coarsen, and elongated, inter-lath cementite may be formed. These can provide potent crack nucleating sites in conditions where the matrix yield strength is still high, and may produce " 350°C embrittlement" either combined with, or in the absence of, segregation of trace impurity elements to prior austenite grain boundaries. Similar effects have been observed in a simple Fe-0.6C steel (King, Smith and Knott 1977). Tempering, or stress-relieving, in the range 615 - 680°C , removes the transformation dislocation density and allows recrystallisation, to a fine ferrite grain size, to occur; carbides generally spheroidise and coarsen, although the presence of "free Mo", in particular, can produce a degree of secondary hardening or, at least, resistance to softening. It is important to appreciate the effect of austenitising temperature in this respect. Up to about 1150°C , molybdenum carbides do not dissolve appreciably in austenite; the grain size remains small, because the boundaries are pinned; and virtually no Mo is available for carbide formation on subsequent tempering. Above 1150°C , the grains coarsen rapidly, because the molybdenum carbides dissolve, Mo is retained in solid solution on rapid cooling, and rather more hardening can occur on tempering (see also Tait and Knott 1977).

The factors controlling cleavage fracture in as-quenched, auto-tempered martensitic or low-carbon bainitic microstructures have not been fully established, although it is fairly clear that the cleavage facet size is related to the packet size. For ultra-low carbon bainitic steels, Brozzo et al. (1977) proposed a relationship between σ_F and the inverse square-root of packet diameter, based on a simple Griffith type of analysis, but the required value of the effective work of fracture was extremely high ($\gamma_p \sim 120\text{Jm}^{-2}$) and no physical model to support this high value was proposed. Knott (1980) suggested that an upper bound to γ_p in these microstructures could be set by assuming that a crack might have to propagate through an unfavourably oriented packet by a ductile mechanism, involving 45° necking of individual laths, so that the critical value of crack tip C.O.D. was equal to a lath thickness. Use could then be made of the expression, in plane strain: $\gamma_p = 2\sigma_Y\delta$; substituting values typical of moderately low temperatures, $\sigma_Y = 600\text{MPa}$, $\delta = \text{lath width} = 0.14\mu\text{m}$, an upper bound for $\gamma_p = 170\text{Jm}^{-2}$ is obtained. It is tempting to assume that the high value for γ_p obtained by Brozzo et al. (1977) is indeed associated with a substantial amount of plastic deformation in unfavourably oriented facets, but direct evidence is lacking, because test-pieces unloaded from levels less than K_{IC} do not show precursor microcracks arrested at packet boundaries.

Recently, a study has been made of cleavage fracture in A533B in the as-quenched condition (Bowen and Knott 1984a). In notched testpieces of the size conventionally tested ($B = W = 12.7\text{mm}$), it was found that σ_F was virtually independent of test temperature over the range -160 to -100°C , although it decreased by about 8% at -196°C . There was minimal variation of σ_F with austenitising temperature and hence with prior austenite grain size or packet size. These results tend to discount the importance of packet size with respect to fracture in the as-quenched (auto-tempered) microstructures. Neither lath width (0.12 - $0.14\mu\text{m}$) nor carbide thickness (13 - 14nm) varied for

austenitising temperatures of 900°C and 1250°C , although the packet size changed from $3\mu\text{m}$ to $50\mu\text{m}$ (austenite grain sizes $8\mu\text{m}$ and $130\mu\text{m}$ respectively), but calculations of σ_F could not substantiate that either lath width or carbide size were responsible for the critical microcrack. One major unknown is the magnitude of the local stresses produced by the transformation dislocation array. As for weld metals, it is possible that when the carbides are so small, non-metallic inclusions may provide microcrack nuclei. Some evidence for this is given in the work of Khan et al (1982), but no fractographic proof has yet been obtained by Bowen, although testing in a different orientation (ST) gave rise to much lower values of σ_F at -196°C , associated with thin sheets of MnS inclusions on the fracture surface.

It is interesting to note (Bowen, Hippsley and Knott 1984) that the value of K_{IC} at -120°C (for the TL orientation) is $58\text{MPam}^{\frac{1}{2}}$ in the as-quenched condition, but decreases to $47\text{MPam}^{\frac{1}{2}}$ after tempering for 1h at 290°C , the fracture surface remaining substantially transgranular cleavage (1% intergranular facets, as-quenched : 6% intergranular facets, after tempering). Lath width, packet size and the inclusion distribution are unaffected by this temper. The intra-lath carbides coarsened slightly, (from a mean size 14nm to a mean of 38nm), but even the larger figure would be associated with values of σ_F much higher than those observed experimentally. Possible explanation for the behaviour could rest on the coarsening of inter-packet or intergranular carbides, in combination perhaps with some "carbide rejection" of trace impurity elements. The implication is that in fully-tempered conditions of steels containing significant carbon levels (greater than 0.1%), carbides will be the dominant crack-nucleating sites.

Two-phase microstructures in which both phases are present in comparable volume fractions (say, between 20% and 80% of one phase and 80% to 20% of the other) and are distributed in regions of comparable size, present a specific problem with respect to the characterisation of fracture toughness. One system which has been studied is a combination of upper bainite and auto-tempered martensite in HY80, which may be obtained in the heat-affected-zone (HAZ) of welded joints. This is particularly the case when preheat is applied to the joint to prevent hydrogen cracking, and slows down the rate of cooling. Dolby and Knott (1972) showed that higher volume fractions of the coarser upper bainite induced more brittle behaviour and that large cleavage facets were obtained, traversing each "patch" of bainite, but no detailed study of fracture toughness as a function of bainite content was made. Hagiwara and Knott (1981) confirmed the general effect of coarse upper bainite throughout the transition range and measured values of K_{IC} at -140°C over the range 0-60% bainite. It is clear that fracture toughness cannot be represented as a weighted average of the terminal values, contrary to some suggestions (Hornbogen 1982). Even when standard deviations are calculated for martensite and bainite, the scatter in K_{IC} values for the 40% bainite/60% martensite alloy is much greater than could be expected for normal distributions. Concentrating on the 40% bainite alloy and examining the fracture surfaces of samples exhibiting extreme, high and low, toughnesses, it was clear that high toughness was associated with a large proportion of martensite (small facets) at the critical distance, \bar{X}_a , ahead of the fatigue-crack tip, whereas the low toughness was associated with a high proportion of bainite at the distance, \bar{X}_b . Similar results have since been obtained for mixed martensite/bainite structures in A533B, but the examination has not been exhaustive.

Hagiwara and Knott regarded the extremes as examples of "bimodal" behaviour and drew attention to results in banded wrought steels and in weld metals where bimodal behaviour was observed in notched-bar tests. Such behaviour is not admissible in any micro-mechanical model considering a single, quasi-

as if it were a genuine fracture stress, but it may bear no more relation to the local fracture mechanisms (void initiation and growth) or the RA. than does the U.T.S. The interaction (not necessarily, relationship) between instability conditions and inclusion content is quite subtle. Gross inclusion distributions may affect the location of instabilities, e.g. during forming processes carried out on metal sheet, but it is also the case that, below a certain volume fraction, the instability is quite divorced from the local mechanisms of void growth. The boundary conditions implied in models for ductile fracture must therefore always be examined closely.

Concern with ductile fracture in engineering applications may be divided into two broad areas: forming processes, where large plastic displacements are applied to pieces which do not contain intentional stress-concentrators; and structures, where the applied stresses are kept well below the yield stress in normal operation. Failure in forming operations is usually associated with unexpected localised thinning or necking and design is based on criteria for plastic instabilities in different stress states, modified perhaps to recognise the effects of gross inclusion distributions. In structures, fibrous fracture under normal design loads is conceivable only if large stress concentrators are present, because these allow local strains to be high although the overall strain is small. If the local plastic zone remained small as the crack propagated, an engineering "brittle" fracture could occur, even though the local micromechanisms were of a ductile nature. One example is the fracture of (cold-rolled) aluminium foil containing an initial long crack, particularly in a load-controlled system which does not provide anti-buckling restraint, so that mode III through-thickness separation can occur. The maximum crack-tip-sliding displacement required is then of the order of the thickness of the foil. It is also possible to obtain catastrophic mode I, "valid K_{IC} ", fractures in fracture toughness testpieces of high-strength aluminium alloys and steels, in which the local micromechanisms are of a fibrous nature, albeit dominated by "fast shear" rather than simple void growth and coalescence by impingement ("internal necking").

A second set of problems in structures involves assessment of the possibility of catastrophic failure under overload or accident conditions. Much of the debate concerning the safety-case for the pressure vessel in the proposed British PWR has, for example, concentrated on highly unlikely transients, such as the shock cooling which would be experienced when cold water floods the vessel to compensate for a loss-of-coolant accident (LOCA). Two situations could be envisaged: one, in which the separation was completely fibrous at the microstructural level; the other, in which growth of the fibrous fracture induced a change to cleavage micro-mechanisms. It is important to view any given application in the correct perspective and this includes geometry, loading system, and material (inclusion content, work-hardening characteristics etc.). There are extremes of behaviour which could engender pessimism for any other situation, but it is important to be aware of the particular factors which lead to each type of extreme behaviour. Some of these are described below.

Consider first the failure of a violin string, of steel wire 1mm in diameter, when it is over-tautened. The event is catastrophic in nature, the broken halves fly apart with violence, there is usually no prior warning of failure, there is no gross stress-concentrator, and yet the fracture mode is fibrous, exhibiting marked local necking. Here, the situation is that the wire is hard-drawn (with a yield strength perhaps of order 1-2 GPa), possesses no ability to work-harden, and the loading system is load-controlled and uniform. When the instability point is reached (at the yield point, which is now identical to the U.T.S.), all the stored elastic energy is released and

provides kinetic energy to the broken halves. Macroscopically, the fracture is brittle, because the maximum plastic displacement (following instability) is only 1mm (assuming necking to a point on 45° slip-lines) i.e. a strain of 0.1%, whereas the elastic strain at instability (for a yield stress of 1 GPa) is $\sigma_y/E = 1/200 = 0.5\%$. The situation is catastrophic (yet ductile on the microscopic scale): this is why safety factors on components such as wire ropes and cables are so high and why suspension cables have a twisted, multi-stranded construction to introduce redundancy (alternative load-bearing paths).

A second situation concerns the failure of rather thin (25mm thick) model pressure vessels (Nichols 1964), containing extremely long, artificial cracks, sealed to prevent leakage of the pressurising medium. Above the transition temperature, hydraulic loading produced crack-arrest, because water is relatively incompressible and crack extension caused the pressure to drop. Pneumatic loading, however, gave rise to catastrophic failure, because the cracks ran more rapidly than the air pressure was released. The material was a structural steel with reasonable work-hardening capacity, but the main features here were the presence of artificially long (0.3 - 0.5m length), through-thickness, sealed cracks in rather thin sections subjected to a "soft" loading system which additionally allowed out-of-plane deformations (bulging) to occur. The situation is analogous to the fracture of aluminium foil containing a long precrack. In general, defects produced during fabrication of a component which is subsequently examined non-destructively, are unlikely to exceed 25-50mm in size and growth to lengths of order 0.3-0.5m, even by fatigue or stress-corrosion mechanisms, would be unlikely to occur under service loadings. In thin-walled vessels, the pressurising medium would leak out before the critical length was reached: in thick-walled vessels, even if a growing "thumbnail" crack "snapped through" the final ligament, the crack would be unlikely to extend catastrophically along the axis of the vessel, because massive bulging and mode III shear would be so difficult to accomplish. The greatest concern is with respect to the adventitious introduction of extremely long cracks in a structure already subjected to pressure loading. Examples are the penetration of a buried gas pipeline by a bulldozer shovel or of a submarine hull by foreign-body impact.

The processes which cause a growing fibrous crack to change to the cleavage mode are by no means clear. One possibility, in load control, is that the crack accelerates and raises the strain-rate ahead of its tip, so that cleavage fracture is produced as a result of the local elevation of yield stress. In notched-bend specimens tested under displacement-control, however, Smith (1973) was able to show that the central fibrous thumbnail increased more slowly with applied displacement rate as it became longer, because the formation of shear lips exerted a "drag" on the crack growth process. He demonstrated that the dominant effect was one of increasing constraint as the ligament beneath the crack tip deformed under conditions equivalent to those in testpieces having longer and longer precracks. Smith's specimens however, failed after general yield and the conclusions possibly do not apply to structures loaded under quasi-elastic conditions. To prevent the change to cleavage, it is clearly advantageous to try to utilise steels with low transition temperatures or, in the case of a LOCA, to try to maintain "upper shelf" conditions at all times, but it is often difficult to be satisfied that these conditions really will be met in service, particularly for thick sections. Fracture toughness tests on full-thickness specimens give a conservative result, but cannot be carried out on irradiated material: on the other hand, defects in service should be small, so that the local triaxiality is low, and results obtained using full-thickness, deep, cracks may be unduly pessimistic.

In addition to these examples of conditions that could produce catastrophic

failure in structural steels as a result of fibrous fracture mechanisms, it has already been stated that a number of high-strength alloys fracture under "valid" K_{IC} conditions, despite exhibiting fracture surfaces which are of a fibrous nature at the microstructural level. The following section is therefore concerned with a description of the fibrous fracture process at the microstructural level, to indicate the differences in behaviour between low-strength and high-strength alloys; and to show how the crack-tip ductility may be affected, not only by the inclusion distribution, but also by changes in matrix properties induced by heat-treatment or prestrain.

FIBROUS RUPTURE AND FAST SHEAR

As in uniaxial specimens, the processes of fibrous fracture in precracked testpieces involve the initiation, growth and coalescence of voids, but these processes now occur in a region subjected to a steep strain gradient and significant hydrostatic stress. The region is surrounded by material subjected to lower strains and this prevents any general plastic instability if the fracture process zone is small compared with the uncracked ligament. The "valid K_{IC} " behaviour of high-strength alloys is therefore associated with microscopic instabilities and the local strains involved represent the material's inherent ductility in the appropriate stress-state.

A useful model situation to consider is that of a crack in a free-machining, mild steel, containing cylindrical MnS inclusions, and cut transverse to the rolling direction so that the configuration is that of a two dimensional distribution of circular inclusions. On application of strain, a plastic zone is produced at the crack tip, allowing it to blunt by the formation of slip-steps which develop a stretch zone. As the strain is increased, the first MnS particle is enveloped and a void begins to grow almost immediately, because MnS particles have virtually no cohesion with the matrix. The strain is increased, further crack blunting and crack tip advance occur, the void increases in size, and other voids begin to grow around more distantly-spaced inclusions. Eventually, the crack tip and the first void coalesce. This is the point of initiation, characterised by a critical crack tip opening, δ_i , and a (symmetrical) stretch-zone width (szw) approximately equal to $\delta_i/\sqrt{2}$. The initiation C.O.D. is then dependent on inclusion size and spacing and on the work-hardening characteristics of the matrix. A model due to Rice and Johnson (1970) gives a functional relationship between (δ_i/X_0) and (X_0/R_0) , where X_0 and R_0 are inclusion spacing and radius respectively, and experimental results (Knott 1977) show that the predictions provide a useful upper bound to crack-tip ductilities for a number of structural steels containing equiaxed inclusions. The model is based on void growth and coalescence in the triaxial stress field ahead of a long crack under plane-strain conditions, for material containing a single distribution of weakly-bonded inclusions. It cannot therefore be expected to apply generally to other microstructures, containing more than one distribution of second-phase particles, which are likely to possess different degrees of particle/matrix interfacial bonding, and, perhaps, different aspect ratios.

It is of interest to treat the processes involved in "fast shear" decohesion. The inclusions in high-strength alloys are usually small and widely-spaced, and two variants of "fast shear" may be obtained, depending on the work-hardening characteristics of the matrix. For HY80 and A533B steels in the fully tempered state (yield stress approx. 500MNm^{-2}), fibrous fracture involves, as for low strength steels, the initiation of a void on a non-metallic inclusion ahead of the crack tip and its growth in the triaxial stress field. Final coalescence with the blunting crack tip does not occur by the simple internal necking mechanism, however, because the strains in the

necking ligament become sufficiently large to initiate cavities around the tempered carbides in the matrix. The cavities link rapidly to produce shear fractures which follow the directions of maximum shear stress (or strain). For a crack tip which has blunted to a semi-circle, these are arcs of logarithmic spirals. In higher strength steels, such as fully tempered HY130 (yield stress approx. 950MNm^{-2}), the voids formed on inclusions do not grow to any marked extent and crack blunting is extremely small, at the stage at which shear fracture is initiated in the matrix. The directions of maximum shear stress are now at steep angles to the line of crack extension and the fibrous fracture follows a "zig-zag" path. Similar effects are observed in high strength aluminium alloys and in QT structural steels tempered at low temperatures. The crack-tip ductility is now controlled by the strains required to initiate fracture at the fine-scale particles which are an integral feature of an alloy's heat-treated microstructure, and factors which affect these initiation strains are segregation of impurities to particle/matrix interfaces, chemical composition of the particle, particle shape, and dislocation content of the matrix, produced by transformation or prestrain. A second effect of prestrain is generally to remove the ability of the matrix to work-harden, so that the fracture process is confined to a single, narrow band of deformation. This clearly reduces the value of δ_i . It is arguable that similar localisation of flow could be produced by neutron irradiation damage.

At the microstructural level, the increase in strain in the ligament between a blunting crack tip and an expanding void may be visualised as an increase in the dislocation density tangled around second-phase particles. The dislocations exert stress on the particle and on the particle/matrix interface: alternative possibilities are that the particle fractures, shears or decoheres from the matrix. In this last case, a condition for decohesion may be set (Knott 1980b) as

$$n\bar{b} = 2\sqrt{2} \{ d(1 - \nu^2) \gamma_I / \pi E \}^{1/2} (d/c)^{1/2} \quad (5)$$

where the particles have radius c and spacing $2d$, n is the number of dislocations, of Burgers vector \bar{b} , tangled around each particle, and γ_I is the work-of-fracture of the particle/matrix interface. The number of dislocations, and hence δ_i , is therefore dependent, *inter alia*, on γ_I . The importance of this parameter was demonstrated convincingly and elegantly by King (King and Knott 1981) who made measurements of δ_i in a quenched and tempered low-alloy steel, given the following heat-treatments: a) tempered for 18h at 480°C plus 1h at 610°C ; cooled rapidly to room temperature; b) tempered for 1h at 610°C , held for 18h at 480°C ; cooled to room temperature. The aim of the second heat-treatment was to allow trace impurity elements, such as P, Sn or Sb, to segregate to intra-granular particle/matrix interfaces (as well as to grain boundaries) and alter the value of γ_I , without altering values of c , d or yield stress. A strong effect was observed, in that δ_i was reduced from 0.075mm to 0.03mm as a result of the segregation heat-treatment. It must be emphasised that the modes of fracture in both cases were fully fibrous, with large voids centred on non-metallic inclusions and small voids formed around the carbide particles.

The general result has been confirmed in a similar set of experiments carried out by Hippsley and Druce (1983), who obtained a decrease in J_{IC} from 200 to 100kJm^{-2} , and who were able to show further, using Auger analysis, that P was present on the surfaces of carbides after the segregation treatment. Interesting observations were also made on the area fractions of large (inclusion-centred) voids observed on the fracture surface. In non-segregated material, the area fraction was large, indicating that the large voids had

grown to substantial size prior to "shear linkage"; i.e. the inter-void strains were large. In segregated material, the area fraction was smaller, because less inter-void strain was required to initiate the "shear linkage".

Effects of tempering on the crack-tip ductilities of quenched-and-tempered structural steels ($< 0.25C$) are broadly similar to those in higher-carbon ($0.25 - 0.4C$) forging steels. As indicated in Table I, values of δ_i increase markedly with tempering temperature. Examples of cracks in the $650^\circ C$ and $350^\circ C$ tempers are shown in figs. 4 and 5 respectively.

TABLE I. Values of δ_i at Different Tempering Temperatures

Steel	δ_i, mm (1h $350^\circ C$)	δ_i, mm (1h $650^\circ C$)
Q1(N)	0.05	0.20
HY 130	0.045	0.12
A533B	0.015	0.09
NiCrMo forging steel	0.02	0.08

Data courtesy C.P. You (Q1(N)/HY130), P. Bowen (A533B) and S. Slatcher (NiCrMo steel).

Two factors may contribute to the low δ_i values obtained for low tempering temperatures as discussed by Slatcher and Knott (1981, 1984) for forging steels. First, there is a high transformation dislocation density which may exert stress on auto-tempered or tempered carbides and thereby reduce the number of dislocations required to be introduced by the applied strain to initiate the "shear linkage" failure. Secondly, the carbides produced by the early stages of tempering are not spheroidal in shape. Intra-lath carbides are generally very small (approx. 14nm width in as-quenched A533B, increasing to approx. 38nm width after tempering for 1h at $290^\circ C$), and it is presumably difficult to nucleate voids on them, but elongated, inter-lath carbides are also produced, and it is arguable that they crack, to produce a microvoid nucleus, under the influence of small matrix strains. The fibre-loading mechanism may operate. Some evidence for this micro-voiding has been given for forging steels (Slatcher and Knott 1981; King and Knott 1981), but its relevance in QT structural steels is not fully established. It is interesting to note that the observations of Schwalbe and Backfisch (1977) indicate that the average dimple size on fracture surfaces obtained from K_{IC} testpieces of a NiCrMo steel decreased for tempering temperatures of order $300-350^\circ C$. If the "linkage" strain had been reduced, this could be attributed to a decrease in the size of the large (inclusion-initiated) dimples, for reasons similar to those invoked by Hipsley and Druce (1983) for their embrittled material. Cracking of elongated carbides to produce an easy form of "shear linkage" may also occur in upper bainite microstructures in structural steels (Chipperfield and Knott 1975; Knott 1982), and it is here that the distinction between "shear linkage" and microcracking becomes unclear. A useful diagnostic piece of information in this respect is the path followed by the fine-scale "linkage" - whether along directions of maximum shear stress (initiation-dominated) or normal to maximum tensile stress (microcrack-dominated).

Studies made by Chen (Chen and Knott 1981) in high-strength 7000 series ($Al_6Zn_2.2Mg_1.8Cu$) aluminium alloys emphasise the importance of the chemical composition of the so-called "dispersoid" particles, with respect to "fast shear" fibrous fracture. Second-phase particles in high-strength aluminium

alloys are generally of three types: inclusions, containing mainly iron and silicon, and having sizes upwards of $1\mu m$; dispersoids, which are inter-metallics in the size range $0.05-0.5\mu m$; and ageing precipitates, which may be only $10-20nm$ diameter at peak hardness. Work by Garrett (Garrett and Knott 1978) has emphasised the general importance of dispersoids with respect to the "shear linkage" process. In Chen's work, attention was paid to two 7000 series alloys (approx. $Al_6Zn_2.2Mg_1.8Cu$), in which Fe and Si were both maintained at $< 0.1\%$ to prevent the occurrence of gross inclusions, but which had different elements added to effect grain refinement. In one case (7475) Cr was added: this gives E-phase dispersoids ($Al_{18}Cr_2Mg_3$) which are somewhat angular and have sizes in the range $0.1-0.5\mu m$. The second alloy (7010) had additions of Zr: this forms the tetragonal phase $ZrAl_3$, which remains semi-coherent with the matrix for sizes up to $0.05\mu m$ at which size it was present in the alloy. It is rather difficult to define completely comparable heat-treatments or strength properties in commercial aluminium alloys, but, following the analysis of fracture toughness in duralumin (Garrett and Knott 1978), critical K_{IC} values (derived from δ_i values) were compared at constant values of $n\sigma_y^2$, where n is the work-hardening exponent. The 7010 (Zr-treated) alloys were found to be significantly tougher than the 7475 (Cr-treated) alloys and this behaviour could be attributed to the fact that the E-phase dispersoids in 7475 crack or cavitate more easily than the $ZrAl_3$ dispersoids in 7010. It is possible that the $ZrAl_3$ particles eventually shear, rather than crack or decohere, but this was not confirmed experimentally. The main point is that the effective value of γ_i in equation 5) has been altered by changing the chemical composition of the particle. An effect of this type might also be observed in secondary hardening steels, tempered to the same yield strength on each side of the secondary hardening peak. Below the peak, the matrix carbides will be cementite or chromium carbide: above the peak, they will contain elements such as Mo, V or W, and this change in composition could alter the value of δ_i , or, indeed, values of K_{IC} for cleavage fracture at low temperature.

It is important also to appreciate the factors that may give rise to degradation in a material's resistance to fibrous crack propagation, particularly with regard to service conditions. Low tempering temperatures (cf Table I) may be taken to represent improper stress relief: operation at high temperatures may produce subsequent reductions in δ_i at room temperature as a result of segregation at operating temperature or of changes in the chemical compositions of second-phase particles. In austenitic stainless steels, precipitation of the brittle intermetallic, sigma phase, may occur as a result of prolonged holds at service temperature. In chemical reactors made of $2\frac{1}{2}Cr_1Mo$ steel where segregation of trace impurity elements may occur at the operating temperature of approx. $500^\circ C$, it is important to control the combination of pressure and temperature on re-pressurisation following a change of catalyst, to avoid high stresses at low temperature; here both the transition temperature and the fibrous fracture resistance could be affected. The deleterious effect of cold prestrain has been mentioned above and some experimental results are given in Table II (Knott 1980b). In mild steel and austenitic steel (Chipperfield 1976), the effect of prestrain appears to be simply to reduce work-hardening capacity, but in QT structural steels, it is possible that the dislocations introduced by cold work subject the tempered carbides to local stress, so that the subsequent strain required to produce cracking or decohesion is reduced: under these circumstances, the concept of an "exhaustion of (local) ductility" may be tenable. In practice, it is vital to recognize that any cold work (pipe-stretching, cold bending, rivetting, the reaming of holes) may severely reduce crack-tip ductility.

TABLE II. Effect of Uniform Cold Prestrain on δ_i

Nominal Prestrain %	δ_i (HY80) mm	δ_i (En32B) mm	δ_i (A533B) mm	δ_i (316) mm
0	0.12	0.09	0.18	0.375
5	-	-	-	0.175
10	0.08	0.05	0.06	-
15	-	-	-	0.125
20	0.04	0.02	-	-
30	-	-	-	0.1

Data from Clayton and Knott (1976): HY80; Willoughby (1979): En32B; courtesy N.W. Ringshall/D.J.H. Corderoy: A533B; Chipperfield (1976): 316.

There are similarities between uniform prestrain and neutron irradiation in terms of increasing a material's yield stress and decreasing its work-hardening rate, so that it might be expected that irradiation damage would also produce decreases in δ_i . In detail, irradiation hardening is produced mainly by point defects, rather than dislocation arrays, so that effects with respect to stressing particles or affecting the interfacial work-of-fracture will not be identical, but the use of uniform prestrain to simulate irradiation is worth exploring, because surveillance specimens have to be small, to fit into a reactor core; and simulation could perhaps be used to establish effects of size on toughness properties. In terms of yield stress, a uniform prestrain of 10% in A533B is roughly equivalent to a (low temperature) neutron dose of $3 \times 10^{22} \text{ n m}^{-2}$, reducing a " K_{IC} " value from approx. 200 MPam^{3/2} to approx. 130 MPam^{3/2} (Knott 1982c).

EFFECTS OF CRACK LENGTH AND SHAPE ON FRACTURE

A crucial feature of both cleavage microcracking and void growth micromechanisms is the effect of the triaxial stress state ahead of the crack tip. Two main aspects of effects of triaxiality may be recognized: first, in attempts to ensure that toughness results and transitional behaviour obtained in small testpieces can be related to "valid" K_{IC} or "plane-strain" J_{IC} or δ_c parameters; secondly, in the application of "valid"/"plane strain" results to defect assessment in structures, where defect lengths are usually small compared with the size of the cross-section and where the defects usually possess a "thumbnail" shape. In the former case, the concern is that small testpieces do not provide sufficient constraint: in the latter, it is found that J_{IC} or δ_i values tend to lead often to over-conservative predictions. It is for this reason that recourse is made to "R-curve" assessments, although it is unlikely that the enhancement of toughness observed during (deep) crack growth in a standard test can, in any rigorous sense, be equated to the behaviour of shallow cracks in service.

Effects of notch depth on transitional behaviour in small testpieces may be explained (Knott 1969, 1973) in terms of the maximum local triaxialities (stress intensifications) that can be generated at general yield. For shallow notches, gross-section yielding limits the maximum stress intensification that can be obtained. In ultra-high strength steels, it has been shown (King and Knott 1980; Wiltshire and Knott 1981) that K_{IC} apparently remains constant with reduction in (a/W) ratio in SEN-bend testpieces, until "top surface" yielding is observed. This may be a fortuitous result, because short cracks are associated with both an increase in local crack-tip ductility and larger plastic zones. These two factors tend to affect the fracture load in opposite

senses, and the net effect in terms of the "R6" design route has been discussed by Wiltshire and Knott (1981).

Effects of stress state on δ_i in fully-plastic testpieces of HY80 steel, have been reported by Hancock and Cowling (1980). Roughly an order-of-magnitude increase in δ_i was found on changing from the fully-constrained Prandtl field to an SEN tensile specimen loaded along a line through the centre of the ligament. An attempt to explain the results in terms of the effect of hydrostatic stress on void growth was made, but it was concluded that this effect, by itself, was insufficient and a postulated change in strain distribution with testpiece geometry was also invoked.

It is instructive to examine recent results (Table III) obtained by You, who has studied effects of (a/W) ratio on the toughness of Q1(N) and HY130 steels, tempered to different strength levels. At -196°C, there is no effect of (a/W) on K_{IC} , even for values as low as (a/W) = 0.05 (a = 1mm). The value of $R_{IY} = 0.16 (K_{IC}/\sigma_Y)^2$ is 0.16mm (σ_Y at -196°C = 1450 MPa); the fracture load (for a/W = 0.05) was 67.0 kN and the load required to yield the top-surface of the testpiece would be 145kN. Fracture is therefore taking place under fully constrained conditions for all crack lengths in the range investigated.

TABLE III. Effects of (a/W) ratio on K_{IC} and δ_i in Q1(N) and HY130 steels

Steel	(a/W) = 0.5	(a/W) = 0.2	(a/W) = 0.1
HY130 T 1h 350°C K_{IC} , MPam ^{3/2} - 196°C	46.0	40.8	41.7 (0.05)
HY130 T 1h 350°C δ_i , mm R.T.	0.045	0.055	0.15
HY130 T 1h 650°C δ_i , mm R.T.	0.12	0.15	0.30
Q1(N) T 1h 350°C δ_i , mm R.T.	0.052	0.053	0.16
Q1(N) T 1h 650°C δ_i , mm R.T.	0.20	0.43	0.56

Data courtesy C.P. You

At room temperature, however, in generally-yielded testpieces, substantial effects of (a/W) ratio on δ_i are observed: for all strength levels, roughly a factor-of-three increase in δ_i is obtained as (a/W) is decreased from 0.5 to 0.1. Effects on J_{IC} would be expected to be up to 25% smaller (because the constraint factor in bending decreases from 1.26 to 1.0 as (a/W) decreases to zero) but still significant. The main cause for the increase in toughness again appears to be the effect of hydrostatic stress on void growth, but it is intriguing that the factor-of-three is observed also for the "fast shear" mode, (e.g. the 350°C tempers) suggesting that hydrostatic tension, or a high maximum principal stress, also facilitates shear linkage. If these observations on fully-yielded testpieces apply equally to thick-section structures (which do not undergo general yielding when subjected to normal service loading), it is apparent that the scientific basis for the over-conservatism found when applying the results of deep-crack fracture toughness tests to defect assessment is associated with effects of stress state on fibrous fracture initiation, rather than any apparent increase of toughness

with crack growth.

The final points concern the behaviour of semi-elliptical ("thumbnail") cracks compared with through-thickness cracks. In ultra-high strength steels (maraging, 300M), the values of K_{IC} , for a "fast shear" mode, were approx. 20% higher if the cracks were semi-elliptical rather than through-thickness (Wiltshire and Knott 1981, King and Knott 1981), but You has obtained values identical to within a few percent, for HY130, tempered at 350°C and tested at -196°C, at which temperature the fracture mode was transgranular cleavage. In the HY130 steel at room temperature, it was much more difficult to grow the crack by fibrous mechanisms along the top surface than it was in the depth direction (You and Knott 1982). The deformation field on the top-surface is equivalent to that for a centre-cracked plate and so the triaxiality is low: the crack has to open by a combination of pairs of in-plane shears (inclined at approx. $\pm 45^\circ$ to the line of crack extension) and out-of-plane, mode III, shears.

Interesting results are also obtained in the transition range. By measuring stretch-zone widths, it can be shown that, once the toughness is reasonably high, the onset of cleavage is controlled by the depth direction (where triaxiality is high) rather than by the top surface: indeed, towards the top of the range, a shear lip is formed on the top surface as a result of the cleavage-crack tunnelling and spreading laterally (fig. 6). Again, subject to the applicability of these observations to large structures, the inference to be drawn is that, for a transient such as a loss-of-cooling accident (LOCA) in a pressurised water reactor, in which a thumbnail crack may be subjected to stress gradients by shock cooling to temperatures of order 35°C (at which temperature, K_{IC} may well be close to 100 MPa \sqrt{m}), there is very little likelihood of the crack "unzipping" along the surface to produce an extended crack. This has important consequences for defect assessment, because the critical value of crack length is decreased by a factor of $(1.12/0.7)^2 = 2.5$ by any such "unzipping".

It is clear that a proper understanding of effects of crack depth and shape could enable a much more rigorous, and, hopefully, less over-conservative, approach to be taken with respect to the assessment of critical defect size in service. The new results are interesting and give cause for optimism, but it is necessary for similar experiments to be carried out on larger pieces before the design engineer, trained only in quasi-LEFM analysis, will be convinced.

ACKNOWLEDGEMENTS

Thanks are due to Professor R.W.K. Honeycombe F.R.S. for provision of research facilities and to members of my research group, particularly P. Bowen, D.E. McRobie, D. Neville and C.P. You for useful discussions and permission to make use of unpublished results.

REFERENCES

- Bowen P. and Knott J.F. (1984a). Metal Science, **18**, p225.
 Bowen P. and Knott J.F. (1984b), submitted for publication.
 Bowen P., Hipsley C.A. and Knott J.F. (1984). Acta Met., **32**, p637.
 Brozzo P., Buzzichelli G., Mascarzoni A. and Mirabile M. (1977). Metal Science, **11**, p123.
 Chen C.Q. and Knott J.F. (1981). Metal Science, **15**, p357.
 Chipperfield C.G. and Knott J.F. (1975). Metals Technology, **2**, p45.

- Clayton J.Q. and Knott J.F. (1976). Metal Science, **10**, p63.
 Costin L.S. and Duffy J. (1979). J. Eng. Mater. Tech. (ASME H), **101**, p258.
 Curry D.A. (1978). Nature, **276** p.50.
 Curry D.A. and Knott J.F. (1976). Metal Science, **10**, p1.
 Curry D.A. and Knott J.F. (1978). Metal Science, **12**, p511.
 Curry D.A. and Knott J.F. (1979). Metal Science, **13**, p341.
 Dolby R.E. and Knott J.F. (1972). J. Iron & Steel Inst., **210**, p857.
 Evans A.G. (1983). Metall Trans., **14A**, p1349.
 Evensen J.D., Lereim J. and Embury J.D. (1977). "Toughness Characterization and Specification for HSLA and Structural Steels" ed. P.L. Manganon Jnr. Met. Soc. AIME p187.
 Fearnough G.D., MSc Thesis, University of Manchester 1972.
 Garrett G.G. and Knott J.F. (1978). Metall. Trans., **9A**, p1187.
 Green G. (1976). PhD Thesis, University of Cambridge.
 Groom J.D.G. and Knott J.F. (1975). Metal Science, **9**, p390.
 Hagiwara Y. and Knott J.F. (1981). Proc. 5th Intl. Cong. on Fracture, Cannes, ed. D. Francois et al., Pergamon p2061.
 Hancock J.W. and Cowling M.J. (1980). Metal Science, **14**, p293.
 Hipsley C.A. and Druce S.G. (1983). Acta Met., **31**, p1861.
 Hipsley C.A., Knott J.F. and Edwards B.C. (1980). Acta Met., **28**, p869.
 Hipsley C.A., Knott J.F. and Edwards B.C. (1982). Acta Met., **30**, p641.
 Hornbogen E. (1982). Proc. 6th Intl. Conf. on Strength of Metals and Alloys, Melbourne, ed. R.C. Gifkins, Pergamon, p1059.
 Judson P. and McKeown D. (1982). Welding Inst. Intl. Conf. on Offshore Welded Structures, London pP3-1.
 Khan M.A., Shoji T. and Takahashi H. (1982). Metal Science, **16**, p118.
 King J.E. and Knott J.F. (1980). J. Mech. Phys. Solids, **28**, p191.
 King J.E. and Knott J.F. (1981). Metal Science, **15**, p1.
 King J.E., Smith R.F. and Knott J.F., Proc. 4th Intl. Conf. on Fracture Waterloo ed. D.M.R. Taplin, Pergamon p279.
 Knott J.F. (1966). J. Iron & Steel Inst., **204**, p104.
 Knott J.F. (1967a). J. Iron & Steel Inst., **205**, p966.
 Knott J.F. (1967b). J. Mech. Phys. Solids, **15**, p97.
 Knott J.F. (1969). Proc. 2nd Intl. Conf. on Fracture, Brighton, ed. P.L. Pratt, Chapman and Hall, p205.
 Knott J.F. (1973). Fundamentals of Fracture Mechanics publ. Butterworths (London).
 Knott J.F. (1977). Proc. 4th Intl. Cong. on Fracture, Waterloo, ed. D.M.R. Taplin, Pergamon, p61.
 Knott J.F. (1980). Metal Science, **14**, p327.
 Knott J.F. (1981). Phil. Trans. Roy. Soc. A299, p45.
 Knott J.F. (1982a) in "Atomistics of Fracture" ed. R.M. Latanision and J.R. Pickens, NATO Advanced Research Institute, Corsica, Plenum p209.
 Knott J.F. (1982b) "Advances in the Physical Metallurgy and Applications of Steels" Liverpool, The Metals Society, p181.
 Knott J.F. (1982c). Proc. 4th European Conf. on Fracture, Leoben, ed. K.L. Maurer and F.E. Matzer, EMAS, **1**, p221.
 McMahon C.J. Jnr. and Cohen M. (1965). Acta Met., **13**, p591.
 McRobie D.E. and Knott J.F. (1984), submitted for publication.
 Neville D.J. and Knott J.F. (1984), submitted for publication.
 Nichols R.W. (1964). Proc. Roy. Soc., **A285**, p104.
 Oates G. (1969). J. Iron & Steel Inst., **207**, p353.
 Pineau A. (1981). Proc. 5th Intl. Cong. on Fracture, Cannes, ed. D. Francois et al., Pergamon, p553.
 Rice J.R. and Johnson M.F. (1970). "Inelastic Behaviour of Solids" ed. M.F. Kanninen et al., McGraw Hill, p641.
 Ritchie R.O., Knott J.F. and Rice J.R. (1973). J. Mech. Phys. Solids, **21**, p395.

Ritchie R.O., Server W.L. and Wullaert R.A. (1979). *Metall Trans.* 10A, p1557.
 Schwalbe K.-H. and Backfisch W. (1977). *Proc. 4th Intl. Cong. on Fracture*,
 Waterloo, ed. D.M.R. Taplin, Pergamon Vol.2, p73.
 Shehata M. and Boyd J.D. (1982). "Advances in the Physical Metallurgy and
 Applications of Steel", Liverpool, The Metals Society p229.
 Slatcher S. and Knott J.F. (1981). *Proc. 5th Intl. Cong. on Fracture*, Cannes,
 ed. D. Francois et al., Pergamon, p201.
 Slatcher S. and Knott J.F. (1984)., this Conference.
 Smith E. (1966). "Physical Basis of Yield and Fracture", Oxford Inst.
 Physics and Physical Soc. p36.
 Smith R.F. (1973). "The Practical Implications of Fracture Mechanisms"
 Newcastle Instn. of Metallurgists Publ. 604-73-Y, p28.
 Tait R.A. and Knott J.F. (1977). *Proc. 4th Intl. Cong. on Fracture*, Waterloo,
 ed. D.M.R. Taplin, Pergamon Vol.2 p671.
 Tweed J.H. and Knott J.F. (1982). *Proc. 4th European Conf. on Fracture*,
 Leoben, ed. K.L. Maurer and F.E. Matzer, EMAS p127.
 Tweed J.H. and Knott J.F. (1983). *Metal Science*, 17, p45.
 Wallin K., Saario T. and Törrönen K. (1984). *Metal Science*, 18, p15.
 Willoughby A.A. (1979). PhD thesis, Imperial College, London.
 Wiltshire B. and Knott J.F. (1981). *Proc. 5th Intl. Cong. on Fracture*,
 Cannes, ed. D. Francois et al., Pergamon, p87.
 You C.P. and Knott J.F. (1982). *Proc. 4th European Conf. on Fracture*,
 Leoben, ed. K.L. Maurer and F.E. Matzer, EMAS p23.

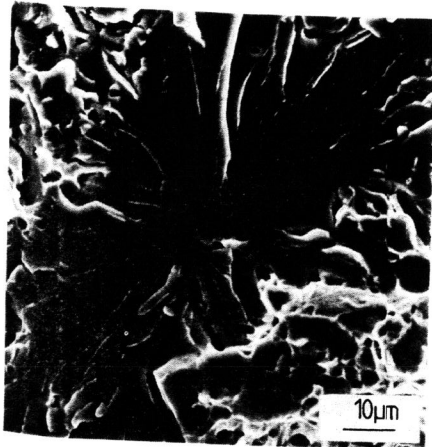


Fig.1 Transgranular Cleavage in C-Mn Weld Metal, initiated from a Non-Metallic Inclusion (courtesy D.E. McRobie)

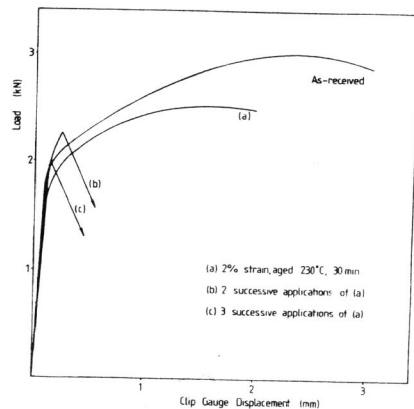


Fig.2 Effect of Strain-Ageing on the Toughness of C-Mn Weld Metal (courtesy D.E. McRobie)



Fig.3 Microcrack in Dual-Phase Steel x 200 x 200 (courtesy D.J. Neville)



Fig.4 Ductile Fracture in HY130 tempered 1h 650°C x 130 (courtesy C.P. You)

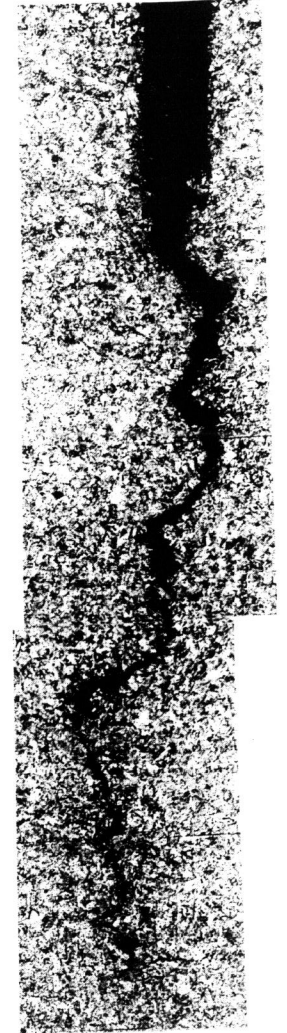


Fig.5 Ductile Fracture in HY130 tempered 1h 350°C x 90 (courtesy C.P. You)

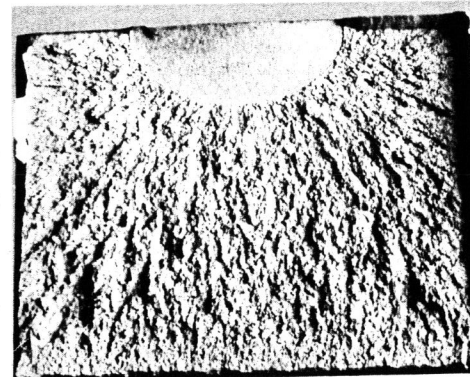


Fig.6 Fracture in "Thumbnail" Crack Specimen. Note shear lip on top surface x 4 (courtesy C.P. You)